Chem. Mater. **2003,** *15,* 2346−2353

Effect of a UV/Ozone Treatment on Siloxane-Containing Copolyimides: Surface Modification and Gas Transport Characteristics

Ho Bum Park, Doo Won Han, and Young Moo Lee*

National Research Laboratory for Membrane, School of Chemical Engineering, College of Engineering, Hanyang University, Seoul 133-791, South Korea

Received January 3, 2003. Revised Manuscript Received April 9, 2003

We have prepared poly(imide siloxane) (PIS) films having various siloxane contents using a two-step polymerization technique and subjected them to a UV/ozone treatment using UV excitation in the range $\lambda = 185-254$ nm to form an SiO_x layer on the surface of the PIS films. From electron spectroscopy chemical analysis (ESCA), we have confirmed that the PDMS surface layer in the PIS films converts into silica as the UV/ozone treatment time increases. Solid-state ^{29}Si NMR provides evidence that the PDMS and silica coexist in the bulk. Gas permeation experiments on non-UV/ozone-treated and on UV/ozone-treated PIS films were carried out using helium (He), oxygen (O_2), nitrogen (N_2), and carbon dioxide (CO_2) penetrants. For PIS films having a high siloxane content (i.e., a volume fraction of 0.457), the UV/ozone treatment decreased the gas permeabilities, but increased the selectivity of several gas pairs owing to the formation of a dense silica layer, which increased with increasing treatment time.

Introduction

Silicones, or polysiloxanes, are popular base polymers of a whole family of organo-silicon compounds that are based on a molecular chain backbone of alternating silicon and oxygen atoms. Of these polymers, poly(dimethyl siloxane) (PDMS) is a commercially available polymer, and the surface properties, interfacial properties, and applications of PDMS are very special. That is, PDMS has a very low surface-energy pendent group (the $-CH_3$ group) that is arranged along the siloxane chain ($-Si-O-$).[1] Many surface modifications of PDMS can be carried out because the siloxane chain allows the methyl group to be orientated to achieve the optimum surface properties. The unique surface properties of PDMS have been attributed to the low intermolecular forces between the methyl groups, the flexibility of the siloxane backbone, the partial ionic nature of the siloxane bond, and the high bond energy of the siloxane bond.[2]

In recognizing the unique surface properties of PDMS, various surface modifications have been utilized to fabricate silicon oxide layers that have a high resistance to oxygen and water and have high gas selectivity. In the case of PDMS, many researchers have attempted to modify the surface of PDMS using ultraviolet (UV) radiation,[3,4] an ultraviolet/ozone (UV/O) treatment,[5] and a plasma treatment.[6] When exposed to UV light or a combination of UV light and ozone, silicone rubbers undergo drastic chemical changes at their surface that are very similar to those induced by oxygen plasma. The oxygen plasma technique penetrates deep under the PDMS surface to a depth of several hundred nanometers and causes irreversible chemical changes in the near-surface region of PDMS,[7] where the PDMS surface is converted onto a thin silica-like layer. Particularly, Koberstein and Mirley have studied and reported many SiO_x fabrication processes using UV/ozone applied at room temperature. Using this simple process, they investigated the site-specific self-assembly of Si/SiO_x nanoparticles on UV/ozone micropatterned PDMS films,[8−11] SiO_x coatings in protecting polymers against photooxidation,[12] and gas separation properties of cross-linked PDMS films after UV/ozone treatment.[13]

In the case of siloxane-containing copolymers,[14] the minimization of the surface free energy leads to an enrichment of the surface with a component that has lower surface free energy−siloxane domains. In particular, poly(imide siloxane) (PIS) copolymers consist of polyimide and PDMS and have a low mixing entropy.

---

* To whom correspondence should be addressed. Tel: +82-2-2291-9683. Fax: +82-2-2291-5982. E-mail: ymlee@hanyang.ac.kr.

(1) Owen, M. J. *Ind. Eng. Chem. Res.* **1980**, *19*, 97.

(2) Owen, M. J. *Silicon-Based Polymer Science*; Zeigler, J. M., Fearon, F. W. G., Eds.; American Chemical Society: Washington, DC, 1990; p 709.

(3) Vasilets, V. N.; Nakamura, K.; Uyama, Y.; Ogata, S.; Ikada, Y. *Polymer* **1998**, *39*, 2875.

(4) Huck, T. S. W.; Bowden, N.; Onck, P.; Pardoen, T.; Hutchinson, J. W.; Whitesides, G. M. *Langmuir* **2000**, *16*, 3497.

(5) Quyang, M.; Yuan, C.; Muisener, R. J.; Boulares, A.; Koberstein, J. T. *Chem. Mater.* **2000**, *12*, 1591.

(6) Ferguson, G. S.; Chaudhury, M. K.; Biebuyck, H.; Whitesides, G. M. *Macromolecules* **1993**, *26*, 5870.

(7) Hillborg, H.; Anker, J. F.; Gedde, U. W.; Smith, G. D.; Tasuda, H. K.; Wilstrom, K. *Polymer* **2000**, *41*, 6851.

(8) Mirley, C. L.; Koberstein, J. T. *Langmuir* **1995**, *11*, 1049.

(9) Mirley, C. L.; Koberstein, J. T. *Langmuir* **1995**, *11*, 2837.

(10) Koberstein, J. T.; Mirley, C. L. US Patent 5,661,092, 1997.

(11) Koberstein, J. T.; Mirley, C. L. US Patent 5,962,079, 1999.

(12) Ouyang, M.; Klemchuk, P. P.; Kobestein, J. T. *Polym. Degrad. Stab.* **2000**, *70*, 217.

(13) Ouyang, M.; Muisener, R. J.; Boulares, A.; Koberstein, J. T. *J. Membr. Sci.* **2000**, *77*, 177.

(14) Yolgör, I.; McGrath, J. E. *Adv. Polym. Sci.* **1988**, *86*, 1.

10.1021/cm030016z CCC: $25.00

This low mixing entropy leads to a microphase-separated structure. A siloxane domain size varies with percentage and block length (in g/mol) of PDMS. As mentioned above PDMS, having low surface energy or surface tension (12−15 dyn/cm), will tend to migrate to the surface of a PIS film to minimize the total free energy of the system.[15−19] The extent of the surface segregation of PDMS in a copolymer depends on numerous factors, such as the bulk composition,[20,21] the block length,[22,23] the annealing process used,[24,25] the casting solvent,[26] and the block sequence distribution.[27]

Zhao et al. have investigated the effect of siloxane segment length on the surface composition of PIS copolymers.[28] They found that both the topmost PDMS surface coverage and the thickness of the surface siloxane-rich layer increased with increasing siloxane segment length in the PIS copolymer. In addition, Mahoney et al. carried out an X-ray photoelectron spectroscopy (XPS) study to determine the effect of incorporating two or more different PDMS blocks lengths (M_w < 1000 g/mol) into the same polymer on the surface characteristics.[29] They synthesized PIS mixtures containing PDMS with average molecular weights (M_n, g/mol) of 252, 440, 550, 703, and 833 for a constant overall siloxane composition of 10%. They concluded that longer siloxane segment lengths resulted in a preferential segregation of PDMS at the surface of the copolymer system.

In this work, we have focused on the surface migration of the PDMS layer in PIS copolymers having various siloxane contents, and then we investigated the effect of a UV/ozone treatment on the conversion of the PDMS layer in the PIS copolymers. To our knowledge, no one has previously investigated the effect of a UV/ozone treatment on the air−polymer interface of siloxane-containing copolymers, such as PIS. We also investigated the conversion efficiency of the silica layer formed from the PDMS surface layer in the PIS copolymer as a function of exposure time, along with the gas transport behavior through these UV/ozone-modified PIS films.

In previous work,[30,31] we have prepared pyrolytic carbon films containing silica from pyrolysis of PIS films having particular surface properties. We found that the carbon−silica films had good gas separation performance. We also found that the initial morphology of the PIS precursor was retained, even after pyrolysis. That is, the PDMS surface layer in the PIS copolymers was mainly converted into a silica layer after pyrolysis. The present work is a continuation of our previous work, and in this paper we report on PIS films in which the top surface is covered by a silica layer formed from a UV treatment instead of the previously reported thermal treatment.[30,31]

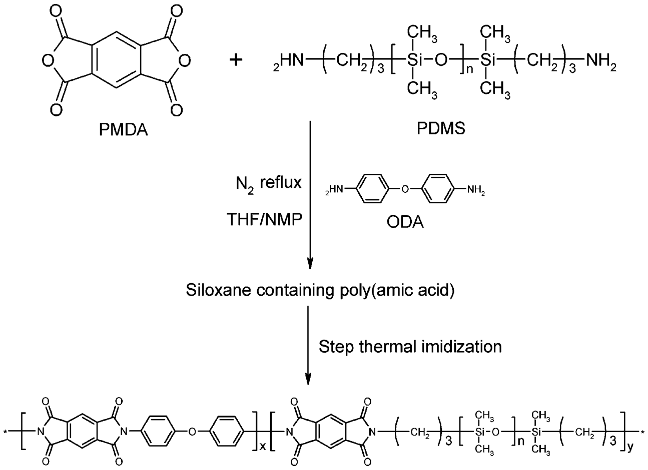

Figure 1. Reaction scheme for the synthesis of poly(imide siloxane).

Table 1. Sample Designation and Composition of the PIS Films

sample code	PMDA (mmol)	ODA (mmol)	PDMS (mmol)	volume fraction of siloxane moiety[a]
PIS I	10	9.8	0.2	0.06
PIS II	10	9.0	1.0	0.27
PIS III	10	8.0	2.0	0.46

[a] Calculated by the group contribution method.

Experimental Section

Materials. The pyromellitic dianhydride (PMDA) and 4,4′-oxydianiline (ODA) used in this work were purchased from the Tokyo Kasei Co., Inc., Tokyo, Japan, and were used as received, without further purification. Amine-terminated poly(dimethyl siloxane) (PDMS) was obtained from the Shinetsu Co., Inc., Tokyo, Japan, and was used after being dried in a vacuum oven at 90 °C for 1 day. The average number of siloxane units in the PDMS was 10, and the value of M_n, determined from gel permeation chromatography, was M_n = 900 g/mol. The *N*-methylpyrrolidinone (NMP) and tetrahydrofuran (THF) used were purchased from the Aldrich Chemical Co., Milwaukee, WI, and dried over a 4-Å molecular sieve overnight before use.

Materials Preparation. Poly(imide siloxane) (PIS) is shown in Figure 1 and was synthesized using a two-step polymerization process. The chemical compositions of the PIS prepared in this study are listed in Table 1. PMDA powders (10 mmol) were added dropwise to each of three THF solutions of PDMS (0.2, 1.0, and 2.0 mmol) under a nitrogen atmosphere, and then the mixtures were stirred for 2 h. The reaction mixtures were added dropwise to NMP solutions of ODA (9.8, 9.0, and 8.0 mmol). The resulting solutions were stirred at room temperature for 6 h to yield homogeneous yellowish siloxane-containing poly(amic acid) (SPAA) solutions. The solid

---

(15) Spontak, R. J.; Williams, M. C. *J. Appl. Polym. Sci.* **1989**, *38*, 1607.
(16) Spontak, R. J.; Williams, M. C. *Polym. J.* **1988**, *20*, 649.
(17) Zhao, J.; Rojstaczer, S. R.; Gardellar, J. A., Jr. *J. Vac. Sci. Technol. A* **1998**, *16*, 3046.
(18) Zhao, J.; Rojstaczer, S. R.; Chen, J.; Xu, M.; Gardellar, J. A., Jr. *Macromolecules* **1999**, *32*, 455.
(19) Zuang, H.-Z.; Gardellar, J. A., Jr.; Incavo, J. A.; Rojstaczer, S. R.; Rosenfeld, J. C. *J. Adhes.* **1997**, *63*, 199.
(20) Chen, X.; Lee, H. F.; Gardella, J. A., Jr. *Macromolecules* **1993**, *26*, 4601.
(21) Chen, X.; Gardella, J. A., Jr.; Cohen, R. E. *Macromolecules* **1994**, *27*, 2206.
(22) Chen, X.; Gardella, J. A., Jr.; Ho, T.; Wynne, K. J. *Macromolecules* **1995**, *28*, 1635.
(23) Chen, X.; Gardella, J. A., Jr.; Kumler, P. L. *Macromolecules* **1993**, *26*, 3778.
(24) Zhung, H. Z.; Gardella, J. A., Jr. *Macromolecules* **1997**, *30*, 3632.
(25) Coulon, G.; Russell, T. R.; Deline, V. R.; Green, P. F. *Macromolecules* **1989**, *22*, 2581.
(26) Thomas, T. R.; O'Malley, J. J. *Macromolecules* **1979**, *12*, 323.
(27) Li, L.; Chen, C. M.; Weng, L. T. *Macromolecules* **1997**, *30*, 3698.
(28) Zhao, J.; Rojstaczer, S. R.; Chen, J.; Xu, M.; Gardella, J. A., Jr. *Macromolecules* **1999**, *32*, 455.
(29) Mahoney, C. M.; Gardellar, J. A., Jr.; Rosenfeld, J. C. *Macromolecules* **2002**, *35*, 5256.
(30) Park, H. B.; Suh, I. Y.; Lee, Y. M. *Chem. Mater.* **2002**, *14*, 3034.
(31) Park, H. B.; Lee, Y. M. *J. Membr. Sci.* **2003**, *213*, 263.

concentration of SPAA was kept at about 10 wt %. The SPAA solutions were then cast onto a glass plate and then thermally imidized at 100 °C for 1 h, 200 °C for 1 h, 300 °C for 1 h, and 350 °C for 1 h under vacuum so as to produce strong, flexible, and dense 15−30-μm-thick films. These PIS films were rinsed with deionized water and stored at 120 °C in a vacuum oven until any residual solvent and/or dust was completely eliminated.

UV/Ozone Equipment. A UV/ozone chamber was used to convert the PIS films. The equipment consisted of a low-pressure mercury-quartz lamp (Korea Ultra-Violet Co., Ltd., Korea), which generated the UV radiation wavelengths of $\lambda =$ 185 and 254 nm, and had an output power of 28 mW/cm^2 at a distance of 6 mm. It is well-known that atomic oxygen is spontaneously generated when molecular oxygen is dissociated by radiation having a wavelength of $\lambda = 185$ nm and that ozone is dissociated by radiation having a wavelength of $\lambda = 254$ nm.[32] Therefore, atomic oxygen was continuously produced and ozone continually generated and diminished when both wavelengths were used. The PIS films were placed at the distance of 6 mm from the UV lamp.

Material Characterization. Non-UV/ozone-treated and UV/ozone-treated PIS samples were characterized using the following analytical methods: the Fourier transform infrared/attenuated total reflectance (FT-IR/ATR) spectra of non-UV/ozone-treated and UV/ozone-treated PIS films were measured using a Nicolet Magna-IR 760 spectrometer ESP in the wavenumber range 500−4000 cm^{-1}. Solid-state ^{29}Si NMR spectra of PIS films before and after UV/ozone treatment were measured using a Varian model NMR 1000 spectrometer to observe the conversion of PDMS domains to silicon oxide on the PIS film surface. A Rigaku Kenki model RAD-C X-ray diffractometer was used to evaluate the crystallinity of UV/ozone-treated PIS samples. Electron spectroscopy chemical analysis (ESCA) was carried out using a Thermo VG Scientific Multilab ESCA 3000 to measure the conversion of PDMS domains to silicon dioxide on the PIS film surfaces. Angle-dependent ESCA data were also obtained to investigate the composition-depth profiles of the modified PDMS domains.

Gas Permeation Apparatus. The gas permeation properties of non-UV/ozone-treated and UV/ozone-treated PIS films were studied. A constant volume, variable pressure method[33] was used to determine the steady-state pure penetrant permeability at 25 °C over a range of upstream pressures up to a pressure of 76 cmHg. A film was loaded into the permeation cell and degassed by exposing both sides of the film to a vacuum. After degassing, the upstream side of the film was exposed to a fixed penetrant pressure (penetrants used = He, CO_2, O_2, and N_2). The steady-state rate of pressure rise on the downstream side was used to determine the permeability coefficient (in units of 1 Barrer = 1 × 10^{-10} cm^3 (STP) cm/cm^2·s·cmHg). At all times during the experiment the downstream pressure was kept below 1 cmHg. In the steady state, when the rate of the downstream pressure rise was constant, the following expression was used to determine the permeability coefficient, P

$$P = \frac{22414Vl}{RTAp_1}\frac{\mathrm{d}p_2}{\mathrm{d}t} \tag{1}$$

where V is the downstream reservoir volume, R is the universal gas constant, T is the absolute temperature, A is the cross-sectional area of the membrane, l is the thickness of the membrane, p_1 is the upstream pressure, and $\mathrm{d}p_2/\mathrm{d}t$ is the rate of change of the downstream pressure. The standard deviation from mean values of the permeability coefficients obtained from at least three times gas permeation experiments was within ca. ±1%. When a mixture of two gases, A and B, is separated, the ideal separation factor for components A and B is defined as the ratio of the permeability of each component as follows:

$$\alpha_{\mathrm{A,B}} = \frac{P_{\mathrm{A}}}{P_{\mathrm{B}}} \tag{2}$$

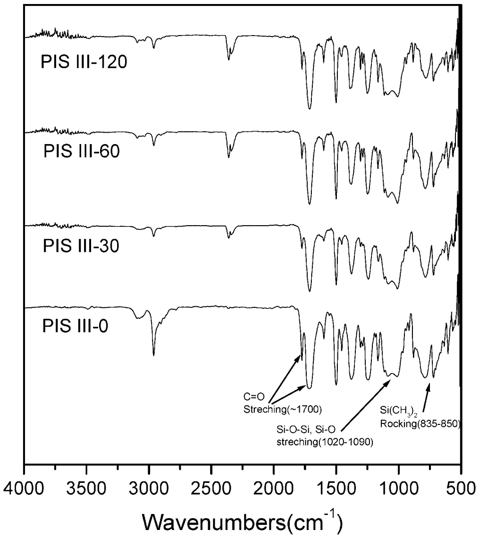

Figure 2. FT-IR/ATR spectra of non-UV/ozone-treated and UV/ozone-treated PIS films.

Results and Discussion

FT-IR/ATR Spectra. The observed degradation and modification of the PIS films from the FT-IR/ATR spectra as a function of UV treatment time is shown in Figure 2. Before we carried out the measurements, we expected that any degradation that took place in the imide segment would be from the decomposition of the carbonyl group in the imide segment to the −OH group on UV irradiation. In addition, as reported in the literature,[32] a UV/ozone treatment of PDMS itself can produce a hydrophilic surface containing −OH groups because the molecular oxygen and ozone generated during the UV treatment can interact with the UV-treated PDMS film. However, the data in Figure 2 do not show any −OH group absorption band arising from the degradation of the carbonyl groups or from the creation of −OH in the PDMS domain in all the samples. The C═O stretch adsorption band occurring around 1700 cm^{-1}, and other imide absorption bands, such as those from C_6H_2 (1165 cm^{-1}) and CNC (1375 cm^{-1}), did not show any large change in absorption. The data from this work lead to the conclusion that the imide backbone is not decomposed by the UV/ozone treatment for treatment times up to 120 min. On the other hand, the intensity of the $Si(CH_3)_2$ absorption band at 835−850 cm^{-1} was reduced considerably by oxidation of the PDMS domains and decreased with increasing UV/ozone exposure time. Commercially available polyimide (Kapton) prepared from PMDA−ODA possesses an excellent chemical and physical resistance toward degradation and loss of material properties when it is exposed to high-energy radiation.[34] This resistance toward high-energy radiation arises because the polyimide contains a high concentration of aromatic groups,

---

(32) Efimenko, K.; Wallace, W. E.; Genzer, J. *J. Colloid Interface Sci.* **2002**, *254*, 306.

(33) Barrer, R. M. *Trans. Faraday Soc.* **1939**, *35*, 628.

(34) Devasahayam, S.; Hill, D. J. T.; Connell, J. W. *Radiat. Phys. Chem.* **2001**, *62*, 189.

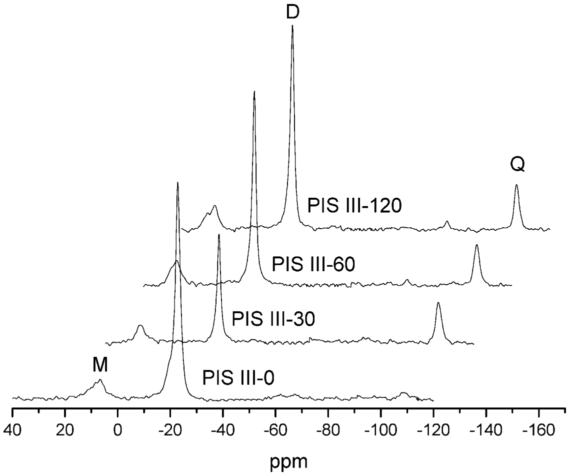

Figure 3. Solid-state ^{29}Si NMR spectra of non-UV/ozone-treated and UV/ozone-treated PIS films.

which can scavenge small radicals, such as hydrogen atoms that can degrade with absorbed energy that excites the vibration states associated with these groups. In this work, we have assumed that only one phase in the main, the flexible dimethyl siloxane domains within the separated two phases, is modified by the UV/ozone treatment and that the rigid imide phase is excluded from being affected by the UV/ozone treatment of the PIS films.

Solid-State ^{29}Si NMR. The modified chemical structure of the PDMS domains in the PIS films from the UV/ozone treatment was determined using solid-state ^{29}Si NMR, as shown in Figure 3. The peaks at 10 and −20 ppm are due to the presence of [Me_3SiO] (M) and [$OSiMe_2O$] (D) in the PDMS domains. The non-UV/ozone-treated PIS Sample III did not show any [SiO_4] (Q) peaks in the NMR spectra at −110 ppm, whereas Q peaks at around −110 ppm were observed in the UV/ozone-treated PIS films, PIS III-30, PIS III-60, and PIS III-120, indicating the formation of silica. Meanwhile, the M and D forms still existed after UV/ozone treatment of the PIS films, which indicates that the PDMS phase had not fully converted into silica because either the exposure time was not sufficient or the silica layer on the converted surface of the PIS films prohibited further conversion of the siloxane phase to silica because the diffusion of oxidative species had become a rate-limiting step.[5,12] Although the solid-state ^{29}Si NMR spectra were not sufficient to deduce quantitatively the amount of modified silica phase, we were able to confirm that the UV/ozone treatment partially converted the PDMS phase into silica.

Wide-Angle X-ray Diffraction. X-ray diffraction is a useful tool for investigating the organization of materials at the molecular level and also provides information on the degree of crystallization of materials. In our work, the crystallinity of the UV/ozone-treated PIS film was evaluated using wide-angle X-ray diffraction. In the case of Samples PIS I and PIS II, any marked change in the X-ray diffraction patterns was not observed with increasing UV/ozone exposure time from 0 to 120 min. These samples showed broad, smooth diffraction patterns, as are typically shown by amorphous polymers. This may be due to the fact that the size, or the cluster size, of the siloxane domains was not large enough to partially orient the converted siloxane phase. The PIS III film, however, exhibited different X-ray diffraction patterns as a function of the UV/ozone exposure time, as shown in Figure 4. In the case of a UV/ozone treatment time of 120 min, the PIS III film showed sharp peaks that were caused by the crystallization or densification of the converted silica phase from the siloxane domains. Therefore, the UV/ozone treatment allowed the PDMS phase to be converted into both amorphous silica and also into partially crystalline silica. This result suggests that the siloxane domain size and content in the siloxane-containing polymer significantly influenced the conversion of siloxane to silica on exposure to UV/ozone.

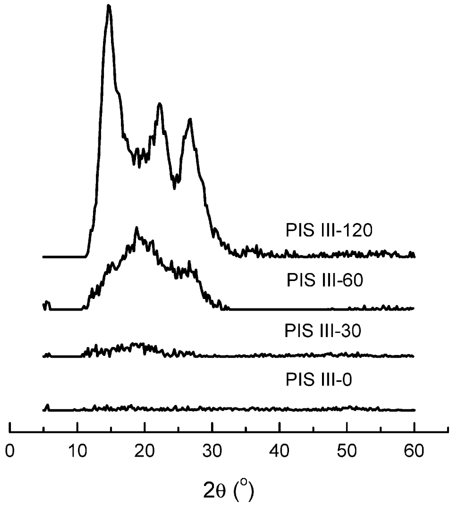

Figure 4. Wide-angle X-ray diffraction patterns of non-UV/ozone-treated and UV/ozone-treated PIS films.

ESCA. Solid-state ^{29}Si NMR and X-ray diffraction provide us with the overall properties of the films, but do not elucidate specific surface properties or provide a depth profile. In many phase-separated copolymeric systems, the thermodynamic driving force for minimizing the total free energy of the system, as well as the bulk composition, block length, processing conditions, and block sequence distribution, results in the preferential surface segregation of the lower surface energy constituent. In particular, siloxane polymers or silicones are usually used as surface-modifying macromolecules by blending them or copolymerizing them with other polymeric architectures, owing to the free rotatability and polarizability of the siloxane bond.[14] Owing to these unique properties, the −Si−O−Si− chain is able to align itself accordingly, resulting in a rich in-depth surface distribution in siloxane copolymers and blends. Thus, some of the most interesting and unique features of siloxane-containing copolymers, such as PIS, are associated with their surface morphology and the resultant surface properties.

In the present study, surface chemical composition analysis was carried out to elucidate changes in the PIS surface composition because UV/ozone exposure would predominately affect the surface properties. Therefore, surface composition analysis of the PIS films, both before and after various UV/ozone exposures, was carried out using ESCA. The Si_{2p} binding energy was used to determine which type of silicon-to-oxygen coordination was present at the surface of the PIS films.

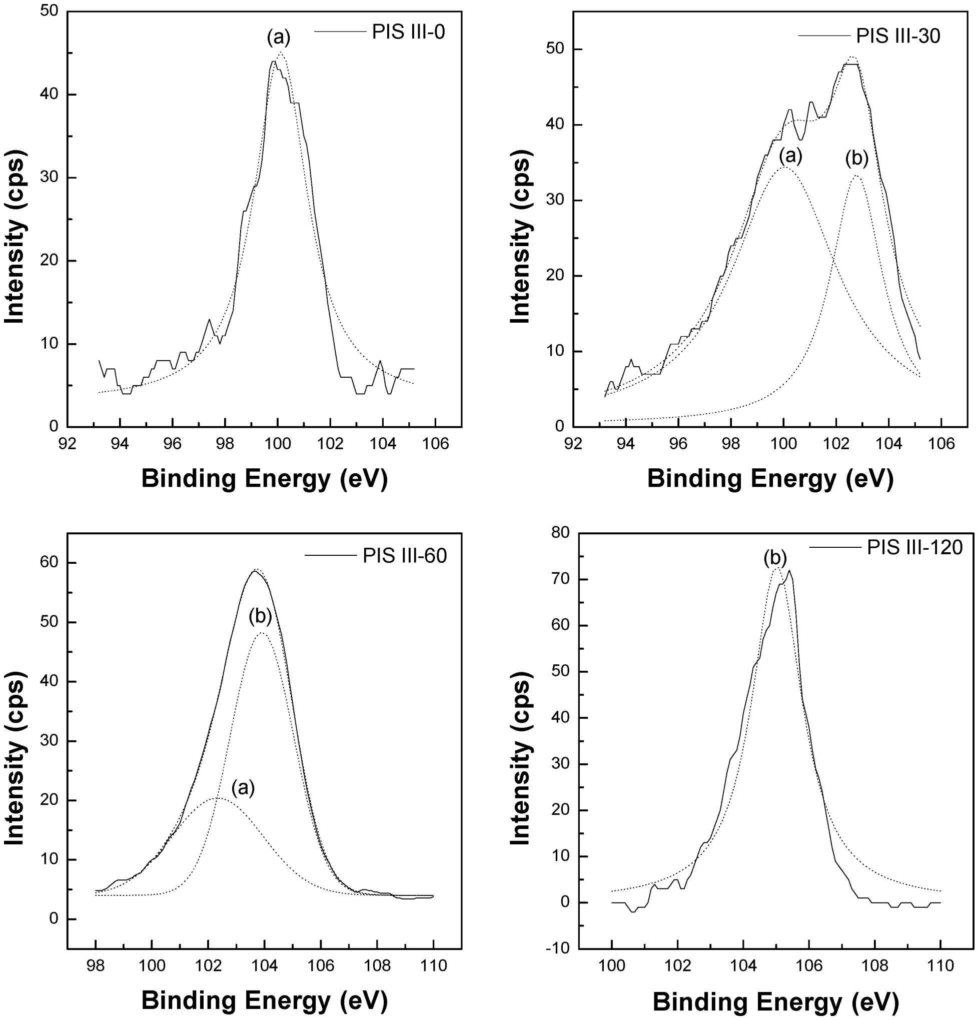

Figure 5. ESCA spectra of non-UV/ozone-treated and UV/ozone-treated PIS films: (a) = main PDMS peak; (b) = main silica peak.

The silicon-to-oxygen configuration has a particular Si_{2p} binding energy that is dependent on the number of oxygen atoms in the coordination shell. Changes in the silicon configuration can therefore be monitored by studying the binding energy.

Figure 5 shows the Si_{2p} binding energy of Sample PIS III. The non-UV/ozone-treated PIS film had a Si_{2p} binding energy of 101.5 eV, indicating the existence of a pure PDMS phase. Usually, the Si_{2p} binding energy increases proportionally as the number of oxygen atoms coordinated to the silicon increases. The Si_{2p} binding energy for Sample PIS III was observed at 101.5 eV, appearing at the particular PDMS binding energy, whereas for Samples PIS III-30 and PIS III-60, the Si_{2p} binding energy had shifted slightly toward higher electron voltages than that of the pure PDMS phase, indicating the existence of partial silica domains. The PDMS Si_{2p} binding energy centered at 101.5 eV was hardly detectable after a UV/ozone treatment for 120 min. ESCA analysis was not sufficient to elucidate all the bulk profiles because ESCA data are integrated over the entire composition of a thin surface layer to a depth of ~10 nm. Therefore, it is inferred that the unmodified PDMS phase still exists in the PIS films after the UV/ozone treatment, especially when considered alongside the solid-state ^{29}Si NMR data. A UV/ozone treatment on various siloxane polymers has been reported to convert a silicone layer into silicon dioxide under atmospheric conditions.[5] This photo-oxidation by UV/ozone is due to the atomic oxygen produced by the in situ photodissociation of ozone, with the photo-oxidation being self-limiting, owing to competition between the rate of diffusion of ozone through the silicon dioxide layer on the surface and the rate of dissociation of the ozone.

Figure 6 shows the Si/C ratio as a function of UV/ozone exposure time. Since silicon species are not volatile, it is assumed that the mass of silicon at the surface does not change. The imide phase consisting of PMDA and ODA was also not decomposed after UV/ozone exposure. An increase in the Si/C ratio is therefore attributed to the removal of carbon species coordinated with silicon. The proportion of SiO_x generated from the PDMS, as determined from the Si_{2p} binding energy, is in good agreement with the Si/C ratio of the polymer. When comparing the results of the Si_{2p} binding energy with the Si/C ratio with UV/ozone treatment time, the oxidation reaction is seen to remove only the organic content of the PDMS phase, leaving a surface composition rich in SiO_x. In the case of Sample PIS III, the films exposed to UV/ozone for 2 h had a much higher Si/C ratio than the PIS III-60 film. This may be due to the fact that the surface of the precursor film was enriched with the PDMS phase, and the carbon in the imide

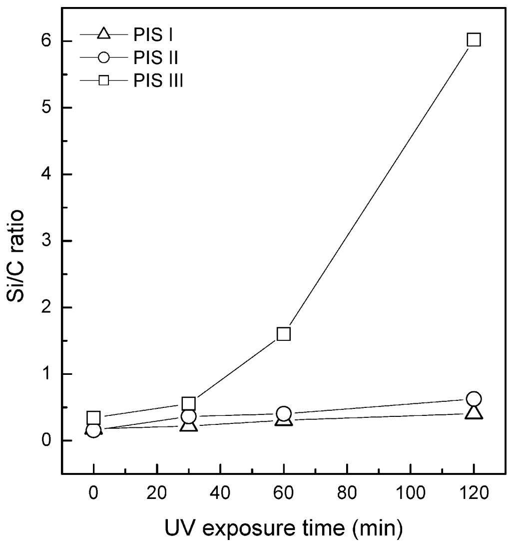

Figure 6. ESCA-determined Si/C ratios of a function of UV/ozone exposure time for Samples PIS I, PIS II, and PIS III.

Table 2. Comparison of the Theoretical and Experimental (ESCA) Surface Compositions of the Polymer Precursor Films Prior to UV/Ozone Treatment

sample code	Si/C experimental and stoichiometric atoms ratios	
	experimental	stoichiometric
PIS I	0.1552	0.0091
PIS II	0.1771	0.0467
PIS III	0.3434	0.0962

phase had little effect on the Si/C ratio, whereas the Si/C ratio of the films of Samples PIS I and PIS II increased linearly, owing to a partial contribution by the carbon atoms of the imide phase. Using this logic, it is presumed that the top surface of the PIS III film was primarily composed of the siloxane phase, while the polyimide phase was the major phase detected on the surface of Samples PIS I and PIS II. A comparison of the theoretical and experimental Si/C ratios of the PIS films is listed in Table 2 as a function of UV/ozone exposure time. When comparing the experimental ratio with the theoretical composition ratio, the experimental Si/C ratios are much higher than the theoretical Si/C ratios for all the PIS films. This is further evidence that siloxane-containing polyimides have a PDMS-enriched surface.

In addition, the conversion efficiency of siloxane into silica was investigated using angle-dependent ESCA measurements, as shown in Figure 7. The photoelectron emission takeoff angles of 60° and 90° were used for the PIS III films. The detectable depth at a photoelectron takeoff angle of 60° was thinner than that of the photoelectron takeoff angle of 90°. The observed Si/C ratio of the photoelectron takeoff angle of 60° was much higher for Sample PIS III-60 compared to the Si/C ratio of the photoelectron takeoff angle of 90°. The magnitude of the change in Si/C ratio narrowed after a UV exposure time of 60 min because the siloxane phase was almost completely converted up to the detectable depth. Thus, after a UV exposure of 60 min, almost full conversion of the silica layer had taken place at the measurement depth for the photoelectron takeoff angle of 60°, but there still existed some unmodified siloxane beyond the detectable depth for the photoelectron takeoff angle of 60°. The Si/C ratio detected for the photoelectron takeoff angle of 90° reached the full conversion to silica value after a UV/ozone exposure time of 120 min. This result can explain the fact that the conversion by UV/ozone exposure takes place on the top surface first, with the conversion process gradually passing from the surface to the inside of the PIS film.

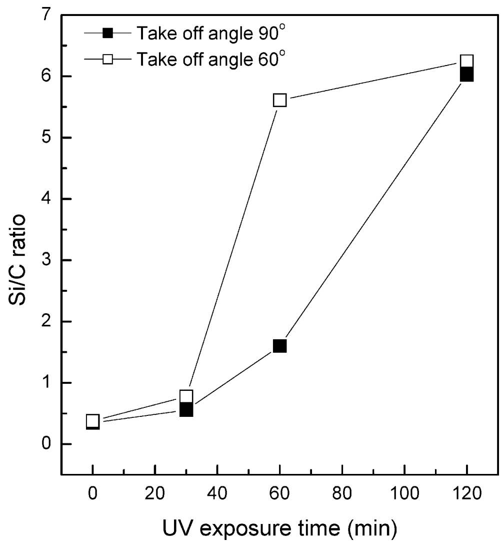

Figure 7. ESCA-determined Si/C ratios as a function of UV/ozone exposure time measured for different photoelectron takeoff angles (60° and 90°).

Gas Permeation Properties. The effect of UV/ozone treatment on the gas transport behavior through the PIS films was investigated in terms of the siloxane content of the PIS films. The gas transport measurements were carried out on a series of non-UV/ozone-treated and UV/ozone-treated PIS film surfaces. Siloxane-containing block copolymers, such as poly(imide siloxane) and poly(amide-imide siloxane), exhibit microphase-separated structures[35] that are composed of microdomains of flexible siloxane segments and of rigid polyimide segments, though diblock copolymers in general do not undergo a macroscopic phase separation since two homopolymers are chemically combined in a diblock system. In rigid−flexible block copolymers, the characteristics of both domains for gas permeation can be very different. The permeation of gas molecules occurs favorably through microdomains of flexible segments, whereas the more rigid segments provide an obstacle to the permeation of gas molecules.

In previous studies,[36−38] we have shown that the gas permeabilities through poly(imide siloxane) and poly(amide-imide siloxane) films containing different siloxane compositions showed specific exponential permeation behaviors, indicating that there existed a percolation threshold for gas permeation at around a 0.2−0.3 volume fraction of the siloxane moiety. This means that the morphological features of these block copolymers are very different at this siloxane content threshold. Thus, three PIS films containing different siloxane contents

---

(35) Arnold, C. A.; Summers, J. D.; Chen, Y. P.; Bott, R. H.; Chen, D.; McGrath, J. E. *Polymer* **1989**, *30*, 986.

(36) Park, H. B.; Ha, S. Y.; Lee, Y. M. *J. Membr. Sci.* **2000**, *177*, 143.

(37) Ha, S. Y.; Park, H. B.; Lee, Y. M. *Macromolecules* **1999**, *32*, 2394.

(38) Lee, Y. B.; Park, H. B.; Shim, J. K.; Lee, Y. M. *J. Appl. Polym. Sci.* **1999**, *74*, 965.

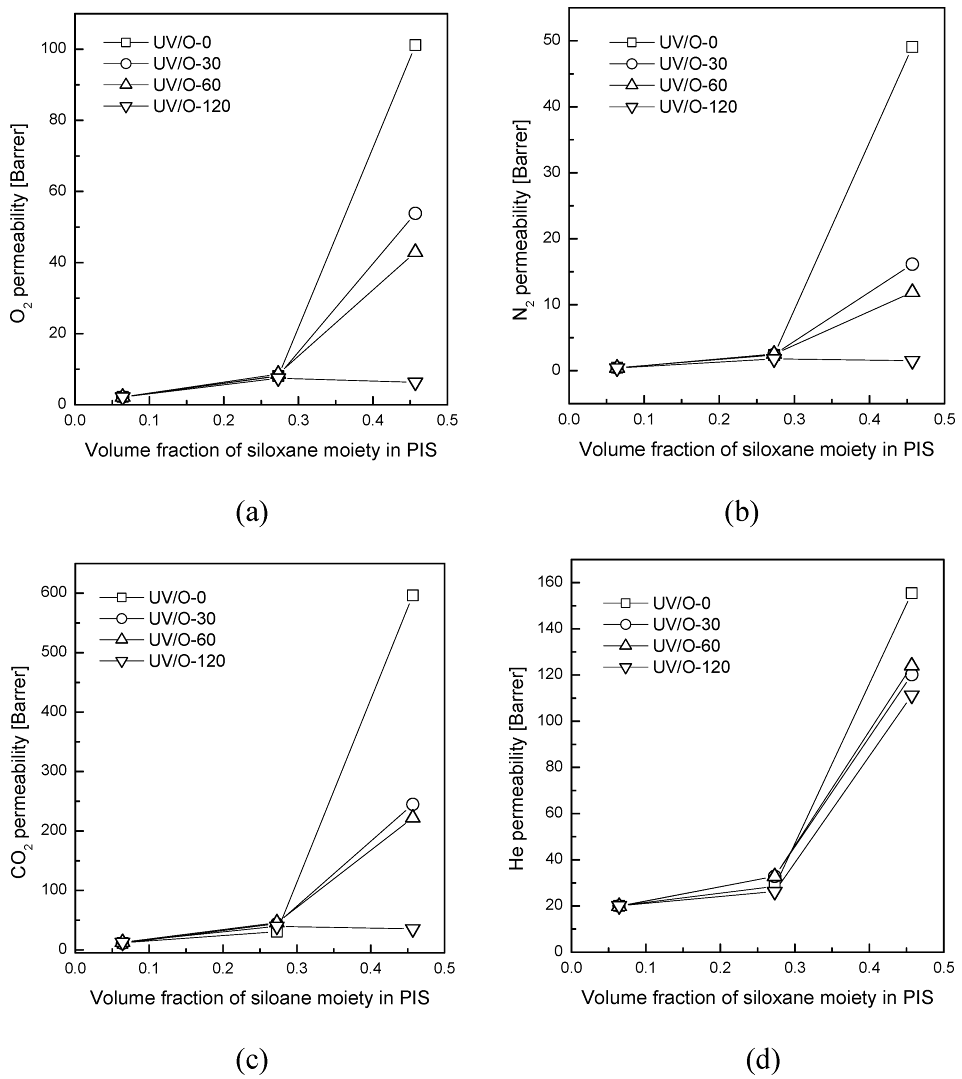

(a) (b)

(c) (d)

Figure 8. Gas permeability versus volume fraction of siloxane moiety in PIS films for various UV/ozone exposure times.

were designed and prepared, with the volume fraction of siloxane moieties in the PIS copolymers being 0.064 (PIS I), 0.273 (PIS II), and 0.457 (PIS III).

Figure 8 shows the permeabilities of O_2, N_2, CO_2, and He through non-UV/ozone-treated and UV/ozone-treated PIS films. In the case of the non-UV/ozone-treated PIS films, all the gas permeabilities increased drastically at around a 0.273 volume fraction of siloxane moiety. This indicates that the volume fraction of the siloxane domain was not large enough to provide connections with each other below the 0.273 volume fraction threshold.[37,38] Therefore, the permeability through PIS of these films is similar to that of polyimide itself.

However, as the UV/ozone treatment time increased, the rate of increase in permeability of all the gas through the UV/ozone-treated PIS films as a function of siloxane content considerably reduced, except for the permeability of He. That is, Sample PIS III containing a siloxane volume fraction of 0.457 showed the largest reduction in gas permeability after the UV/ozone treatment. After a UV/ozone exposure time of 120 min, the gas permeabilities through the PIS III film (except for He) were smaller than those of the non-UV/ozone-treated PIS II film. This means that the surface of Sample PIS III (having the highest siloxane content) was covered mainly by a PDMS layer and that, after UV/ozone exposure for 120 min, most of the PDMS layer at the surface was converted into silica, which acted as a barrier to gas transport. In general, UV, UV/ozone, and plasma treatments of pure PDMS films lead to a decrease in gas permeability.[39−41] This is largely attributable to the formation of an oxidized SiO_x-rich surface layer. However, in the case of He gas, a lower reduction in permeability was observed after the UV/ozone treatment. This can be explained by the pore sizes being large enough to transport such a small atom as He (atomic radius 2.60 Å) existing in the silica layer after the UV/ozone treatment. (Note that the He/N_2 selectivity of the PIS III film increased to 74.2 after UV/ozone exposure for 120 min.)

The dependence of the gas permeabilities and selectivities of PIS films on the UV/ozone exposure time is summarized in Tables 3, 4, and 5. For Sample PIS I, no large change in gas permeability was observed, and the He/N_2, O_2/N_2, and CO_2/N_2 selectivities were observed to increase only slightly. For low siloxane-content Sample PIS I, the PDMS layer did not fully cover the surface of the PIS film. In addition, the polyimide main

---

(39) Houston, K. S.; Weinkauf, D. H.; Stewart, F. F. *J. Membr. Sci.* **2002**, *205*, 103.

(40) Oh, S.-J.; Zurawsky, W. P. *J. Membr. Sci.* **1996**, *120*, 89.

(41) Bhide, B. D.; Stern, S. A. *J. Membr. Sci.* **1991**, *62*, 37.

Table 3. Gas Permeation Results of Non-UV/Ozone-treated and UV/Ozone-Treated PIS I Films Measured at 25 °C

			UV/ozone exposure time (min)			
sample		penetrant	0	30	60	120
PIS I	permeability [Barrer][a]	He	20.06	19.99	19.87	20.11
		CO_2	11.86	11.23	12.90	12.87
		O_2	2.22	2.20	2.18	2.16
		N_2	0.44	0.42	0.42	0.40
	selectivity	He/N_2	45.6	47.6	47.3	50.3
		CO_2/N_2	27.0	26.7	30.7	32.2
		O_2/N_2	5.1	5.2	5.2	5.4

[a] 1 Barrer = $10^{-10} \times$ cm^3 (STP) $cm/cm^2{\cdot}s{\cdot}cmHg$.

Table 4. Gas Permeation Results of Non-UV/Ozone-Treated and UV/Ozone-Treated PIS II Films Measured at 25 °C

			UV/ozone exposure time (min)			
sample		penetrant	0	30	60	120
PIS II	permeability [Barrer][a]	He	28.4	32.8	32.8	26.2
		CO_2	30.7	44.0	45.6	39.6
		O_2	8.1	8.2	8.7	7.5
		N_2	2.4	2.4	2.5	1.8
	selectivity	He/N_2	12.0	13.5	13.1	14.7
		CO_2/N_2	12.9	18.0	18.2	22.2
		O_2/N_2	3.4	3.3	3.5	4.2

[a] 1 Barrer = $10^{-10} \times$ cm^3 (STP) $cm/cm^2{\cdot}s{\cdot}cmHg$.

Table 5. Gas Permeation Results of Non-UV/Ozone-Treated and UV/Ozone-Treated PIS III Films Measured at 25 °C

			UV/ozone exposure time (min)			
sample		penetrant	0	30	60	120
PIS III	permeability [Barrer][a]	He	155.4	120.2	124.0	111.3
		CO_2	596.4	244.8	222.3	35.3
		O_2	101.2	53.8	42.9	6.3
		N_2	49.1	16.2	11.9	1.5
	selectivity	He/N_2	3.2	7.4	10.4	74.2
		CO_2/N_2	12.2	15.2	18.7	23.5
		O_2/N_2	2.1	3.3	3.6	4.2

[a] 1 Barrer = $10^{-10} \times$ cm^3 (STP) $cm/cm^2{\cdot}s{\cdot}cmHg$.

matrix was not much affected by the UV/ozone treatment. In the PIS II film, the gas permeabilities and selectivities both increased up to an exposure time of 60 min, but after an exposure time of 120 min, the gas permeabilities and selectivities began to decrease. The reduction in gas permeability is consistent with the formation of an SiO_x-rich surface layer. The cause for the decrease in gas pair selectivity is less certain, but is likely to be attributable to the inhomogeneous nature of the surface layer modification, and possibly to defects being formed during extended treatment times.

Conclusions

In this study, we have designed and prepared PIS films having various siloxane contents and have investigated the effect of UV/ozone on the surface modification of the PIS films. We found that the UV/ozone treatment converted the surface of the PIS films into silica, which was due to the surface of the PIS films being PDMS-rich. As the UV/ozone exposure time increased, the top PDMS layer at the PIS film surface was fully converted into a silica layer, which was confirmed by ESCA. In addition, the UV/ozone treatment converted the PDMS phase into amorphous and partially crystalline silica in PIS films containing a high siloxane content. This suggests that the siloxane domain size and the bulk composition of the siloxane-containing polyimide mainly influence the conversion of siloxane to silica by the UV/ozone treatment. The gas permeabilities of PIS films containing a low siloxane content did not show any significant change from normal films, but the selectivities of various gas pairs did increase slightly. On the other hand, the gas permeabilities of PIS films containing a high siloxane content decreased, and the selectivities of gas pairs increased with increasing UV/ozone exposure time, implying that the bulk composition of siloxane-containing polyimides significantly influences the gas permeation performance after a UV/ozone treatment.

In conclusion, we can expect that the conversion of a UV/ozone-induced SiO_x layer in various siloxane-containing copolymers and blends will offer specific advantages in gas separation for those processes conducted at elevated temperatures and in oxidative atmospheres where existing organic membranes offer little resistance.

Acknowledgment. We acknowledge financial support from the Korea Institute of Science and Technology for Evaluation and Planning through the National Research Laboratory Program. D.W.H. is very grateful for a BK21 Fellowship from the Ministry of Education, South Korea.

CM030016Z